Electronic Supplemental Information for:

Flexible GaAs solar cells on roll-to-roll processed epitaxial Ge films on metal foils: a route towards low-cost and high-performance III-V photovoltaics

P. Dutta[1,2,3], M. Rathi[1,2,3], D. Khatiwada[1,2,3], S. Sun[1,2,3], Y. Yao[1,2,3], B. Yu[1,2,3], S. Reed[1], M. Kacharia[6], J. Martinez[4], A. Litvinchuk[3], Z. Pasala[5], S. Pouladi[1], B. Eslami[1], J. -H. Ryou[1,2,3], H. Ghasemi[1], P. Ahrenkiel[5], S. Hubbard[6], V. Selvamanickam[1,2,3]

[1] Department of Mechanical Engineering, University of Houston, Houston, TX 77204, USA
[2] Advanced Manufacturing Institute, University of Houston, Houston, TX 77204, USA
[3] Texas Center for Superconductivity, University of Houston, Houston, TX 77204, USA
[4] Materials Evaluation Laboratory, NASA Johnson Space Center, Houston, TX 77085, USA
[5] Nanoscience and Nanoengineering, South Dakota School of Mines and Technology, Rapid City, SD 57701, USA
[6] Department of Physics & Microsystems Engineering, Rochester Institute of Technology, Rochester, NY 14623

Description of R2R PECVD for Ge growth

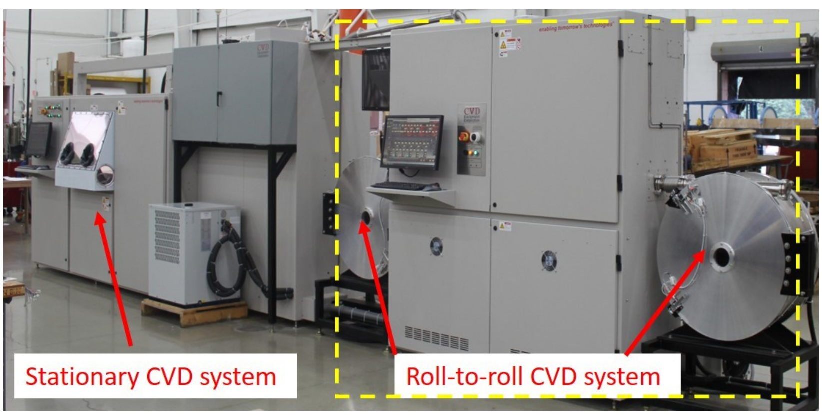

Figure S1. *R2R CVD system custom-designed and developed at U of H to deposit the Ge films continuously on moving metallic foils. The blue arrows show the dispense and take-up spools.*

The custom-designed roll-to-roll R2R-CVD tool for scalable processing of Ge films on moving metallic tapes is shown in figure S1. The spools with substrates are loaded in the cylindrical spool chambers which can hold over a kilometer length of substrates. The tool is designed for multi-pass capability to coat multiple layers needed for device structures, by passing the tape back and forth in the reactor between the spool chambers. A polymeric interleaf film is used to protect the deposited films from contamination. The R2R system is also capable for growth of III-V materials by metal organic chemical vapor deposition. The typical stationary CVD chamber is shown on the left, where all the standard optimization runs are carried out before moving on to the long-length R2R processes.

Dark current vs voltage plots of GaAs PV on sputter and CVD Ge substrate

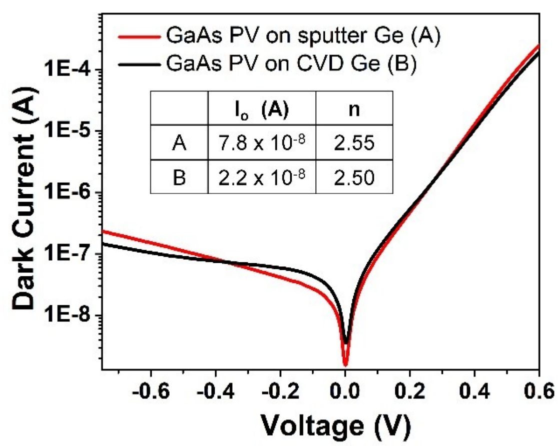

Figure S2. *Dark I-V plots of flexible GaAs solar cells on CVD Ge and sputtered Ge template on metal foil substrates*.

Figure S2 shows the dark current-voltage (I-V) plots of the GaAs solar cells fabricated on CVD and sputtered Ge templates. The reverse saturation currents (Io) were 2.2 and 7.8 x 10^{-8} A and ideality factors 2.5 and 2.55 for GaAs p-n diodes on CVD and sputtered templates, respectively. The I-V curve was fitted with the diode equation $I = Io(e^{eV/nKT} - 1)$ to determine the saturation current (I_o) and ideality factors (n), where

I = current across the diode

I_o = reverse saturation current

V = applied voltage

e = electron charge

k = Boltzmann constant

T = temperature

Illuminated current vs voltage of GaAs PV on CVD Ge substrate

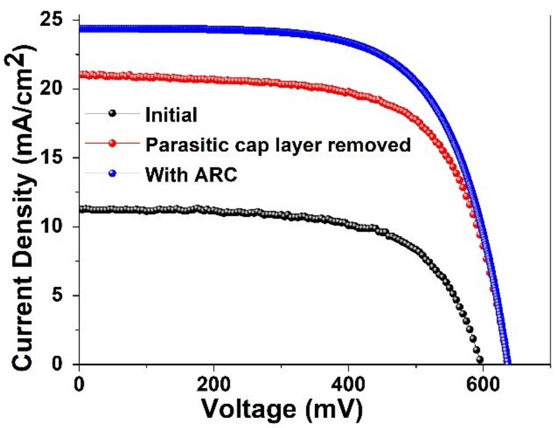

Figure S3. *J-V plots of GaAs SJ solar cell on CVD Ge on metal substrate showing the improvement in device properties with parasitic layer removal and ARC coating*

Table T1: Device parameters of GaAs solar cell on metal substrate

	V_{oc} (V)	J_{sc} (mA/cm^2)	FF (%)	Efficiency (%)
Initial	592	11.4	67	4.3
Parasitic cap layer removed	634	21.0	69	8.8
With ARC	642	23.5	72	10.5
With shadowing adjustment	642	25.0	72	11.5

Figure S3 shows the illuminated J-V plots of a representative GaAs SJ solar cell on metal substrate measured at three stages of device fabrication, as fabricated, parasitic cap layer removed and with final ARC layer. The table T1 shows the device parameters extracted from the J-V plots. The V_{oc} increased from 592 to 642 (50 mV increase) and the J^{sc} increased significantly from 11.4 to 23.5 mA/cm$^{2.}$., resulting in an increase of device efficiency from 4.3 to 10.5 %. The increase of V_{oc} and J_{sc} can be attributed to the passivation of side walls (reduction of recombination) and increased light absorption due to the removal of the parasitic cap layer (30 nm GaAs highly doped layer) and incorporation of ARC coating. The device efficiency increased further when the shadowing effect is taken into consideration and the effective device area was adjusted.

Table T2: Device data of GaAs solar cells on CVD and sputtered Ge template showing results of 3 devices.

GaAs device on CVD Ge template					**GaAs device on sputtered Ge template**				
Device #	Eff (%)	Voc (mV)	Jsc (mA/cm^2)	FF (%)	Device #	Eff (%)	Voc (mV)	Jsc (mA/cm^2)	FF (%)
CVD1	11.5	642	25	72	Sput1	6.7	570	18.6	63
CVD2	8.8	606	19	70	Sput2	5.2	531	15	65
CVD3	6.8	622	18.2	64	Sput3	6.4	571	16.5	66
CVD4	8.1	612	18.5	72	Sput4	6.5	550	17.1	69

Table 1 shows the results of four GaAs devices on CVD and sputtered Ge templates. The first row shows the champion device, as reported in the manuscript. The next two rows show two other devices made during the same period of same size (500 µm dia).

Table T3: Representative device data of GaAs solar cells on sputtered Ge template showing results of 4 different device sizes.

Device ID	**Dia (µm)**	**Voc (mV)**	**Jsc (mA/cm^2)**	**FF (%)**	**Eff (%)**
A	500	549	16.8	72	6.6
B	750	543	15.8	64	5.5
C	1000	542	15	65	5
D	1250	534	15.4	62	5.1

Table T3 shows the effect of device size on the performance of devices on sputtered Ge template. It was observed that with the increase in device size, there was a drop in performance. Here, a decrease in device efficiency from 6.6 % to 5.1 % was observed as the device size increased from 500 to 1250 µm. This trend was observed in general for all devices made on CVD and sputtered Ge templates on IBAD textured metal foils.

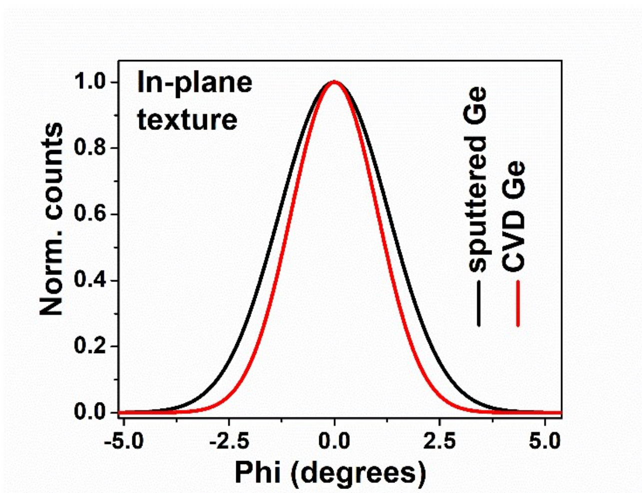

Figure S4. *In-plane phi-scan showing the narrowing of FWHM in CVD Ge film compared to sputtered film indicating improvement in crystalline alignment in CVD Ge films*

The crystalline alignment of CVD Ge in the in-plane direction showed improvement compared to sputtered Ge. Figure S4 shows the normalized counts vs Phi angle plot of CVD and sputtered Ge film. The in-plane texture (peak width or FWHM) were 2.4 and 3 degrees for CVD and sputtered Ge respectively. Decrease in peak width of CVD Ge was observed which indicated enhancement in crystalline alignment in CVD Ge films.